c-kit expression identifies cardiovascular precursors in the neonatal heart

Yvonne N. Tallini[a,1], Kai Su Greene[a,1], Michael Craven[a,1], Alyson Spealman[a,1], Martin Breitbach[b], James Smith[a], Patricia J. Fisher[a], Michele Steffey[a], Michael Hesse[b], Robert M. Doran[a], Ashley Woods[a], Babu Singh[a], Andrew Yen[a], Bernd K. Fleischmann[b], and Michael I. Kotlikoff[a,2]

[a]Biomedical Sciences Department, College of Veterinary Medicine, Cornell University, Ithaca, NY 14853; and [b]Institute of Physiology 1, Life and Brain Center, University of Bonn, 53105 Bonn, Germany

Directed differentiation of embryonic stem cells indicates that mesodermal lineages in the mammalian heart (cardiac, endothelial, and smooth muscle cells) develop from a common, multipotent cardiovascular precursor. To isolate and characterize the lineage potential of a resident pool of cardiovascular progenitor cells (CPcs), we developed BAC transgenic mice in which enhanced green fluorescent protein (EGFP) is placed under control of the c-kit locus (c-kit[BAC]-EGFP mice). Discrete c-kit-EGFP^{+} cells were observed at different stages of differentiation in embryonic hearts, increasing in number to a maximum at about postnatal day (PN) 2; thereafter, EGFP^{+} cells declined and were rarely observed in the adult heart. EGFP^{+} cells purified from PN 0–5 hearts were nestin[+] and expanded in culture; 67% of cells were fluorescent after 9 days. Purified cells differentiated into endothelial, cardiac, and smooth muscle cells, and differentiation could be directed by specific growth factors. CPc-derived cardiac myocytes displayed rhythmic beating and action potentials characteristic of multiple cardiac cell types, similar to ES cell-derived cardiomyocytes. Single-cell dilution studies confirmed the potential of individual CPcs to form all 3 cardiovascular lineages. In adult hearts, cryoablation resulted in c-kit-EGFP[+] expression, peaking 7 days postcryolesion. Expression occurred in endothelial and smooth muscle cells in the revascularizing infarct, and in terminally differentiated cardiomyocytes in the border zone surrounding the infarct. Thus, c-kit expression marks CPc in the neonatal heart that are capable of directed differentiation in vitro; however, c-kit expression in cardiomyocytes in the adult heart after injury does not identify cardiac myogenesis.

bacterial artificial chromosome | progenitor cell | stem cell

The process of early heart cell specification from pluripotent cardiovascular progenitor cells (CPcs) has recently been advanced that a common cardiovascular precursor can give rise to cardiomyocytes, endothelial cells, and smooth muscle cells through directed differentiation of ES cells in vitro, and when these cells are implanted into adult hearts (1–5). Several markers have been reported to identify CPc, including the kinase insert domain protein receptor KDR (also known as Flk-1) (1, 2), the stem cell factor (SCF) receptor c-kit (4–6), the LIM-homeobox transcription factor islet-1 (isl1) (7), and the cardiac transcription factor Nkx2.5 (4). In vitro directed differentiation of ES cells suggests mammalian heart development involves mesoderm specification to a multipotent precursor stage. However, such cells have not been isolated from the heart and shown to undergo multipotent differentiation in vitro, and Nkx2.5 -expressing cells isolated from E7.5 and E8.5 mouse embryos could not be induced to expand and differentiate (4).

Used extensively as a marker to identify adult hematopoietic stem cells, c-kit is expressed during various stages of cell lineage commitment in germ, mast, stellate, epithelial, endothelial, and smooth muscle cells (8–10). Isolated c-kit^{+} cells from E9.5 and E10.5 embryos express cardiac and smooth muscle genes in vitro and differentiate to smooth and cardiac myocytes in vivo (4). Here, we report the isolation and characterization of neonatal c-kit^{+} cells from a transgenic mouse in which enhanced green fluorescent protein (EGFP) expression is placed under control of the *kit* locus

within a bacterial artificial chromosome (BAC). EGFP^{+} cells from postnatal c-kit[BAC]-EGFP mouse hearts expand in culture and differentiate in vitro into cardiac, smooth muscle, and endothelial cells. The study of isolated CPc is likely to provide important information with respect to the genetic status, mechanism of differentiation and commitment, and biological potential of these cells.

Results

Generation of c-kit[BAC]-EGFP Mice. To facilitate the study of heart precursors known to express c-kit (4–6), we inserted the EGFP coding sequence in frame at the start codon of c-kit (1st exon) (11) within a 186-kb BAC by recombineering methods (Fig. 1A) (12). A founder line was identified by a 1.1-kb PCR amplicon that included c-kit and EGFP DNA (Fig. 1 A and B). Neonatal c-kit[BAC]-EGFP pups displayed intense skin fluorescence consistent with the expression of c-kit in melanocytes (Fig. 1C) (10), and were easily distinguished from nontransgenic littermates by using a hand-held fluorescent light source and filtered goggles [see supporting information (SI) *Materials and Methods*]. In adult mice strong EGFP fluorescence was observed in a variety of organs in a pattern consistent with endogenous c-kit expression (Fig. 1D); expression was observed in interstitial cells of the intestines and stomach, muscle layer of the uterus and testis. EGFP was detected by immunochemistry in Leydig cells and outer layer spermatogonium in the testis, in basket and stellate cells in the molecular layer of the cerebellum, and within the hippocampus (Fig. 1E), consistent with the cell-type-specific expression of c-kit in these tissues (13). As expected from a genetic strategy in which the endogenous locus was not altered, c-kit[BAC]-EGFP mice display no apparent phenotype.

Spatial and Temporal Expression of EGFP in the Heart. The expression pattern of EGFP was analyzed in heart sections from embryonic [14.5 and 18.5 days post coitus (dpc)], PN 2–3, and adult c-kit[BAC]-EGFP mice. Fluorescent cells were observed in the atrial and ventricular walls at 14.5 dpc (Fig. 2A Top). The total number of EGFP expressing cells increased as the heart expanded in size, peaking shortly after birth (PN 2–3; Fig. 2A Middle). Thereafter, the number declined rapidly and c-kit-EGFP^{+} cells were only occasionally observed as mononuclear cells within vascular compartments, or rarely as a striated myocytes within the cardiac intersti-

Fig. 1. Generation and evaluation of c-kit^{BAC}-EGFP mice. (A) BAC-targeting the c-kit initiation codon; Neo cassette removed before DNA injection. Arrows indicate PCR genotyping primers. (B) 1.1-kb PCR product in founder (lane 1); water and WT in lanes 2 and 3; 1-kb DNA ladder in lane 4. (C) Bright-field and fluorescent images of PN0 c-kit^{BAC}-EGFP pups. (D) EGFP expression in adult tissues shows predicted pattern of expression. (E) Immunolocalization of EGFP in Leydig and outer region of spermatogonium (arrow) in adult testis, stellate and basket cells in the molecular layer of the cerebellum, and selective hippocampal neurons. (Scale bars: C, 1 mm; D, testis, 1 mm, and others, 100 μm; E, testis, 25 μm and brain, 50 μm.)

tium, in adult mice (Fig. 2A Bottom). In PN hearts EGFP⁺ cells were observed in the atrioventricular region (Fig. 2C), in the atrial and ventricular walls (Fig. 2A), and the epicardial border, where intensely staining cells were often observed (see below). C-kit coexpression was examined by dual immunolabeling of heart sections (Fig. 2B) and in cells sorted by EGFP fluorescence (see below). The coincidence of anti-EGFP and CD117 staining was >90% within clusters (Fig. 2B), but isolated cells often only stained with one of the two antibodies (≈45% coincidence). The latter result may be due to differences in protein half-life, technical issues related to the CD117 antibody, or incomplete transcriptional fidelity of the c-kit transgene.

We examined the lineage and developmental status of c-kit-EGFP cells in postnatal (PN 2–3) hearts by immunostaining tissue sections that retained EGFP fluorescence. In the atrioventricular region, clusters of EGFP fluorescence cells were observed at various stages of cardiovascular development (Fig. 2C). Some cells costained with α-actinin and displayed early cardiac morphology, whereas smaller, elongated α-actinin negative cells that costained with Flk-1, which marks ES cell-derived CPc (1), were also observed (Fig. 2D). The latter group included clusters of cells coexpressing the endothelial lineage marker PECAM1 (Fig. 2E Left). Fluorescent cells were also observed at the epicardial border, which were CD45 positive, indicating hematopoietic lineage (Fig. 2E Center and Right). In some clusters a gradation from less differentiated and more intensely fluorescent, to more striated and weakly fluorescent cells, was observed (Fig. 2F). Quantitative morphometry indicated the more intense staining epicardial cells represented 0.101 ± 0.004% of all heart cells (3,373 ± 330 per heart), whereas nonepicardial EGFP⁺ cells were 0.46 ± 0.14% of all cells (16,044 ± 6,343 per heart). We estimate that EGFP cells constitute <1% (0.56 ± 0.16; n = 6) of all cells in the neonatal mouse heart. Taken together,

these results indicate that the c-kit-EGFP⁺ cell population includes CPc in several stages of development and lineage commitment.

Expansion and Differentiation of Neonatal c-kit⁺ Cells in Vitro. To isolate c-kit-EGFP⁺ expressing cells and determine their potential to differentiate into multiple cell lineages we sorted cells from pooled PN 0–5 c-kit^{BAC}-EGFP hearts. EGFP⁺ cells could be distinguished by FACS from background fluorescence of nontransgenic cells, although there was overlap at the low end of EGFP expression, as shown by the comparison of fluorescence histograms of heart cells from c-kit^{BAC}-EGFP⁺ and WT litter mates (Fig. 3A). Use of a gate that captured cells 5-fold brighter than the mean fluorescence intensity, a subset of cells (sEGFP) could be obtained that included only c-kit-EGFP⁺ cells (Fig. 3A). In some experiments the total pool of c-kit-EGFP cells (tEGFP) was obtained and c-kit-EGFP⁺ cells distinguished from nonexpressing EGFP cells by epifluorescent microscopic examination, whereas in others the sEGFP fraction was used. The total number of sEGFP cells per heart averaged 23,300 ± 3,773 (n = 7) from FACS sort analysis, a finding similar to that obtained by counting cells in individual heart slices (19,418 ± 7,138; n = 6) (Fig. 3B).

tEGFP and sEGFP cell fractions plated on gelatin-coated slide wells expanded, with individual fluorescent cells undergoing cell cycling as indicated by antiproliferating cell nuclear antigen staining (Fig. 3C) and formation of clusters of fluorescent cells from isolated cell populations. Twenty-four hours after plating, sEGFP cell fractions were 100% fluorescent, consisting of small, brightly fluorescent cells containing a small amount of cytoplasm, flat cells with a large amount of cytoplasm, or spindle-shaped cells; after several days in culture, cells increased in size, often forming long processes that contacted neighboring cells (Fig. 3D Left and Center). Cells also expanded when plated on irradiated feeder cells (Fig. 3D Right). The expanding cell population gradually lost expression of EGFP, by 9–16 days after plating of sEGFP cells 67 ± 4% (n = 3) expressed EGFP and many of these cells coexpressed nestin (see below). Cells expanded as clusters with a central clump of EGFP⁺ cells (Fig. 3E) or as flattened cell aggregates (Fig. 3F).

Cells analyzed 24 h postplating lacked expression of the marker CD45, indicating epicardial cells did not survive disaggregation. The endothelial marker PECAM1 was barely detected at 24 h (0.003 ± 0.003%), although cells did induce expression after several days in culture (see below). Approximately one-third of the cells expressed smooth or cardiac muscle-specific proteins at 24 h (39 ± 13% and 30 ± 4%, respectively; Fig. 3G). Nine to 16 days post-FAC sort sEGFP cells displayed smooth muscle, cardiac muscle, and endothelial markers (Fig. 3H). On rare occasions, smooth muscle, troponin T, and c-kit were observed in the same cell demonstrating their bipotential capacity (Fig. 3I). No coexpression of Isl1 and c-kit-EGFP was observed, consistent with separate developmental populations (14) (data not shown). However, >50% of the cells were nestin positive 9 days after initial plating, further suggesting their precursor status (15) (Fig. 3 G and J).

Cardiac Differentiation of c-kit-EGFP⁺ Cells. Several days after plating in media containing basic fibroblast growth factor (bFGF), many c-kit-EGFP⁺ cells began to spontaneously contract. As cells expanded in culture, contractions spread over clusters of EGFP expressing and nonexpressing cells, with initiation occurring in multiple regions and complex rhythmic patterns displayed (Movie S1) or just within EGFP⁺ clusters without spreading to EGFP⁻ cells (Movie S2). Contractions were also observed in single, non-striated EGFP cells after several days in culture (Movie S3, Fig. 4A), indicating ongoing myogenesis (see below).

The electrical phenotype of spontaneously contracting neonatal c-kit-EGFP⁺ cells was examined by patch clamp. Current clamp recordings revealed spontaneous action potentials (APs) with characteristics similar to those previously reported from embryonic, and ES cell-derived, cardiac myocytes (16, 17). The range of AP
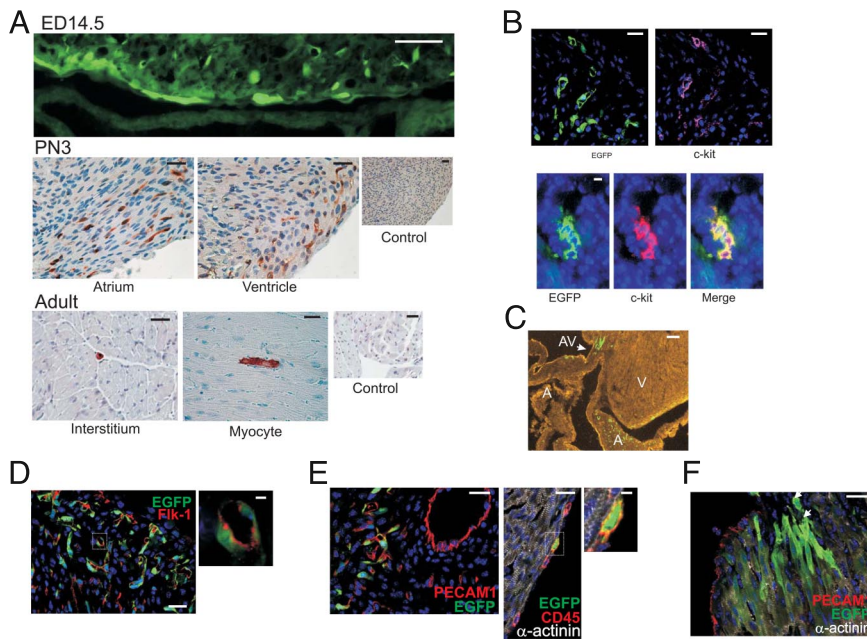
Fig. 2. EGFP expression in c-kit[BAC]-EGFP mouse hearts. (*A*) EGFP expression in the heart wall of 14.5-dpc embryo (fluorescence) and PN 3 (immuno) neonates. In the adult heart rare immunostained cells were observed. Control, no 1° antibody. (*B*) EGFP/c-kit expression concordance. Anti-EGFP (green); anti-CD117 (red). Note lack of coexpression (*Upper*) and colocalization within a niche (*Lower*). (*C*) Native EGFP expression in the atrioventricular region of a PN 2 heart. (*D*) Some cells coexpressed Flk-1 and EGFP. (*E*) Some c-kit^{+} cells coexpress PECAM1, indicating endothelial commitment. Very bright EGFP-expressing cells were commonly observed in the epicardium; these cells commonly coexpressed the hematopoietic lineage marker CD45. (*F*) c-kit-EGFP^{+} cells in the atrioventricular region showing a gradient of EGFP expression, from less differentiated bright cells (arrows), to less fluorescent striated cells. A, atrium; AV, atrioventricular region; and V, ventricle. Hoechst staining (blue) (*B*, *D–F*). (Scale bars: *A*, 14.5 dpc, 50 μm, and others, 25 μm; *B*, 10 μm; *C*, 50 μm; *D*, 25 μm; *D Inset*, 10 μm; *E Left*, 25 μm; *E Center*, 20 μm; *E Right*, 5 μm; *F*, 25 μm.)

morphologies included nodal, atrial, and ventricular characteristics (Fig. 4*B*). Spontaneously depolarizing phase 0 currents and stable resting potential were observed, as well as atrial- or ventricular-like plateau phases and nodal-type transient depolarizations. Phasic electrical activity included both stable depolarization rates and complex, repeated burst-type activity (18). The latter pattern was observed mainly in networked EGFP^{+} cells, and occasionally in single EGFP cells. AP characteristics were summarized based on the level of resting membrane potential (RMP) (Table S1). Group 1 displayed the most depolarized RMP (-46 ± 2.8 mV), the slowest upstroke velocity (dv/dt, 4.4 ± 1 V/sec), and the longest duration (APD^{90}, 123.6 ± 10.5 ms). APs in groups 2 and 3 displayed more stable RMPs (-60 ± 0.6 mV and -75 ± 1 mV, respectively), faster dv/dt (34.5 ± 6.3 and 69.5 ± 9.6 V/sec), and shorter APD^{90} (77.8 ± 7.7 and 66.5 ± 13.9 ms). Significant differences existed between all 3 groups for the parameters mentioned above ($P < 0.05$), with the exception of APD^{90} between groups 2 and 3. No significant difference existed between mean AP frequencies for group 1 (240 ± 34 min^{-1}), group 2 (287 ± 28 min^{-1}), or group 3 (205 ± 30 min^{-1}).

The ion channel dependence of the APs was investigated by using blockers of cardiac fast sodium channels [tetrodotoxin (TTX), 10 μM], and L-type calcium channels (nifedipine, 1 μM). TTX abolished APs in a reversible manner (Fig. 4*C*), indicating the cardiac nature of these currents; nifedipine also inhibited the APs, indicating the importance of L-type Ca^{2+} channels (Fig. 4*D*). Taken together, these data indicate the cardiac phenotype of spontaneously contracting c-kit-EGFP[+]-derived cells.

Lineage Potential of c-kit[+]-EGFP Precursor Cells. To determine whether individual c-kit-EGFP^{+} cells are multipotent, we sorted sEGFP cells and cultured them for 9–16 days under conditions designed to promote cardiovascular lineage differentiation. Wells were stained for cardiac, smooth muscle, or endothelial markers, and the fraction of positive cells counted in all wells. Cardiac differentiation was markedly favored in media containing bFGF, with ≈15% of cells expressing the troponin T, compared with <3% in media containing tumor growth factor-β1 (TGF-β1) or vascular endothelial growth factor (VEGF) (Fig. 5). Addition of VEGF to the media enhanced the expansion of endothelial and smooth muscle cells, and the latter effect was more potent than that observed in TGF-β1 media. TGF-β1, which promotes smooth

muscle differentiation (2, 4), significantly decreased in cardiac myogenesis. Thus, c-kit[BAC]-EGFP cells from neonatal hearts can be manipulated in vitro to selectively expand the 3 cardiovascular lineages.

Because the above results could reflect induced expansion of precommitted cells or selective differentiation of multipotent precursors, we performed limiting dilution studies to determine the fate of individual clonal populations. Cells were plated to yield one cell per well and cultured for 21 days; ≈15% of the individual cells counted on day 3 survived and expanded during the culture period (Fig. 5*B*). Separate immunostaining of the expanded populations revealed individual committed cardiac, smooth muscle, and endothelial cells among cells that did not express these markers (Fig. 5*C*). The above result, in which cells of all 3 lineages were detected, was repeated in 19 separate dilution experiments. Costaining for αSMA and PECAM1 or troponin T and PECAM1 clearly demonstrated smooth muscle and endothelial or cardiac and endothelial lineages arising in clonal expansions (Fig. 5*D*). In vitro expansion of single clones to all 3 cardiovascular lineages indicates that c-kit-EGFP^{+} cells from neonatal hearts include a population of undifferentiated cells similar to ES cell-derived cardiovascular precursor cells (2, 4, 7).

Reexpression of c-kit-EGFP[+] after Injury. To analyze c-kit expression following myocardial injury, we induced cryolesions in the left ventricle of adult c-kit[BAC]-EGFP mice (19). Seven days after cryolesion there was marked expression of fluorescent cells in the infarct and the border zone, with fluorescent cells often associated with vessels within the infarcts, and modestly fluorescent striated cardiomyocytes surrounding the border zone (Fig. 6*A*). In sham-operated mice rare EGFP^{+} cells were equally distributed throughout the myocardium. EGFP expression increased by day 3, peaked at 7 days, and declined at 21 days postinjury.

EGFP^{+} cells within the infarct were found preferentially in contributing to blood vessels (Fig. 6*B Left* and *Inset*). Luminal EGFP cells in vessels were PECAM1 positive (Fig. 6*B Right*), whereas cells surrounding larger vessels stained for α-SMA (data not shown), thus contributing to the endothelium and smooth muscle layer of vessels. Single endothelial cells formed lumens, consistent with early angiogenesis. Fluorescent cells within vessels were still observed 21 days after the lesion. By contrast, the pattern of EGFP expression in the border zone was different, with modest,
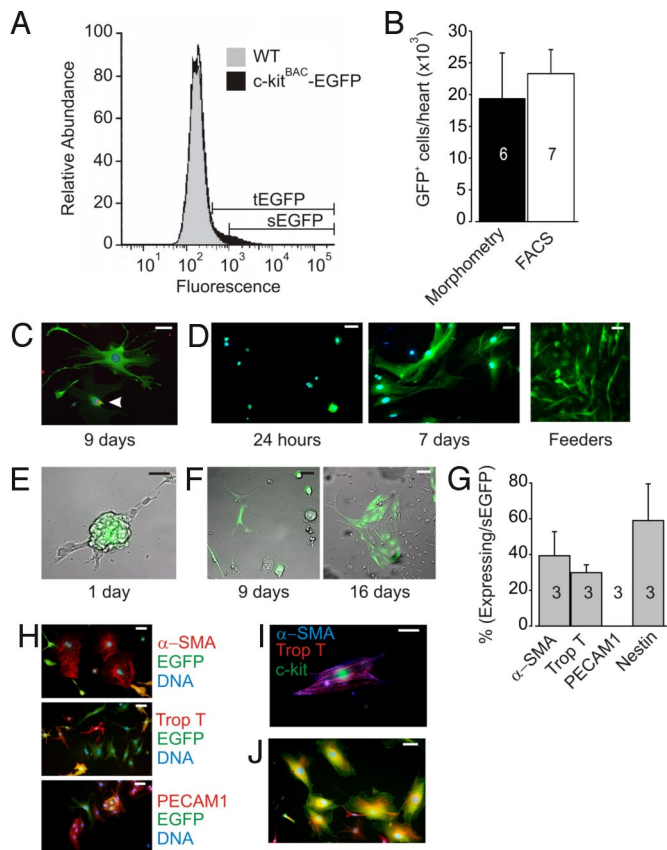
Fig. 3. Isolation and expansion of FACS sorted cardiac c-kit-EGFP cells. (*A*) Representative FACS from PN c-kit[BAC]-EGFP and WT littermate hearts. WT and EGFP histograms were normalized to same maximum. tEGFP overlaps with brightly autofluorescent WT cells; sEGFP identifies a pure c-kit-EGFP$^+$ population of cells 5 times brighter than background fluorescence. (*B*) Morphometry and FACS estimate of EGFP$^+$ cells in neonatal hearts. (*C*) EGFP expression and PCNA (red) staining indicates cycling in c-kit sEGFP$^+$ cells cultured for 9 days in basic media. Arrow indicates PCNA staining. (*D*) EGFP expressing cells at 24 h (*Left*) and 9 days (*Center*) post-FACS. Note differences in cell size and shape. At right tEGFP cells plated on feeders expand rapidly (3 days) in a network pattern. (*E*) Merged bright-field and fluorescent image show after 1 day in culture some tEGFP cells form clusters. (*F*) Images taken from the same field of 9 days (*Left*) and 16 days (*Right*) post-sEGFP$^+$ plating in basic media shows expansion of cells. Images are merged fluorescent and bright field. Some cells at both 9 and 16 days are no longer fluorescent. (*G*) Distribution of committed cells 24 h post-FACS (tEGFP cells). Note lack of endothelial cells (PECAM1) and equal distribution of smooth muscle (αSMA) and cardiac cells (troponin T). Nestin staining suggests a population of undifferentiated cells. Number of experiments is indicated in bars. (*H*) Costaining 9–16 days post-FACS (sEGFP cells). (*I*) c-kit (green) cell expressing both αSMA (blue) and troponin T (red) markers. Merge of αSMA and troponin T yields purple. (*J*) Nestin (red) and c-kit (green) costaining in cells cultured for 9 days. (*H* and *I*) DAPI staining (blue). (Scale bar: *C*, 20 μm; *D–F*, *H*, and *J*, 50 μm; *I*, 10 μm.)

EGFP expression in striated cardiomyocytes (Fig. 6*C*) and robust expression in elongated fibroblasts. EGFP$^+$ cardiomyocytes did not express phosphohistone H3 (pHH3), a marker of cell proliferation, and the number of these cells peaked at day 7 and declined to the level of sham control by day 21 (Fig. 6*D*). Neither mitotic figures nor immature cardiomyocytes were observed postcryoablation. Troponin T-positive cells were never observed within the infarct, indicating a lack of cardiac myogenesis. pHH3$^+$ fibroblasts and leukocytes were observed within the infarct and at the border zone, only $\approx$1% of pHH3$^+$ cells were also c-kit$^+$. Thus, c-kit expression is observed in cells associated with the early revascularization and fibrosis of the infarcted heart, declining within a few weeks after injury, and is also seen in differentiated myocytes, but the latter is not associated with myocyte proliferation.
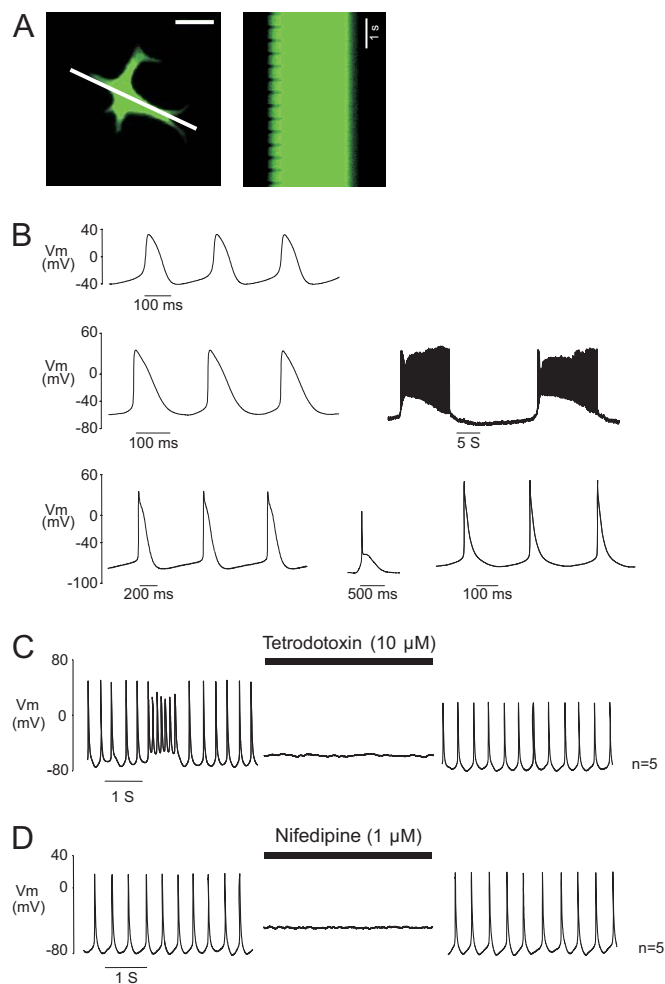

Fig. 4. Cardiac phenotype of spontaneously beating c-kit$^+$-EGFP cells. (*A*) Single, contractile EGFP expressing cell at left in single frame from a time series. Line through image indicates area used for sequential scans of fluorescence shown at right. Left edge of line scan shows rhythmic contraction of the top left cell extension at $\approx$2 Hz. (Scale bar: 25 μm.) (*B*) APs ranged from nodal-like (*Top*), to more atrial (*Middle*) or ventricular (*Bottom*) morphologies. Note prominent diastolic depolarization phases. Networked c-kit-EGFP$^+$ cells fired rhythmical burst-like activity, interrupted by periods of quiescence accompanied by prominent membrane hyperpolarization. (*C*) TTX (10 μM, $n = 5$) or (*D*) Nifedipine (1 μM, $n = 5$), reversibly abolished APs.

Discussion

Recent evidence suggests that within the developing heart a resident population of CPc exists, with the capacity to differentiate into multiple cardiovascular cell lineages (4). C-kit expression appears to characterize a developmental stage of one subset of these cardiovascular precursor cells (1), but studies in mouse (4) and human (2, 3) ES cell-derived precursors suggest that a c-kit-negative stage precedes commitment. To examine the role of c-kit expression in CPcs, and to facilitate their isolation and analysis, we created BAC transgenic mice in which EGFP is placed under the transcriptional control of the c-kit locus to achieve high expression levels and outstanding transcriptional fidelity (20, 21). Bernex *et al.* (22) and Wouters *et al.* (23) knocked reporters into the c-kit locus, but did not examine cardiac expression, and the dominant nature of the c-kit locus complicates this strategy. A minimal c-kit promoter strategy yielded similar results with the concordance of CD117 and anti-GFP staining that declined after birth (24, 25). We show that embryonic and postnatal c-kit$^+$ cells are in a mixed developmental state within the developing heart (Fig. 2), as predicted for a

Fig. 5. c-kit[BAC]-EGFP neonatal heart cells are cardiovascular precursors. (*A*) Modification of commitment outcomes by addition of specific growth factors. Number of experiments indicated in bars. (*B*) Clonal expansion showing a single EGFP[+] cell at day 3 (*Left*) and the clone after 20 days (*Right*). (*C*) Immunostaining of clones from a single EGFP[+] cell after 21 days. Individual cells showing commitment to all 3 heart lineages. (*D*) Coimmunostaining of clonal populations demonstrates commitment to cardiac (*Left*) or smooth muscle (*Right*) and endothelium in the same clone. DAPI staining (blue) in *C*. (Scale bars: *B–D*, 50 μm.)

Fig. 6. Reexpression of c-kit-EGFP after injury in the adult heart. (*A*) (*Left*) Stefanini-fixed heart 7 days postsurgery. Note the large number of EGFP^{+} cells at the border zone and within the infarcted (darker) area. (*Right*) Rare fluorescent cells in sham heart. (*B*) EGFP cells within infarct. (*Left*) Fluorescence wide-field image of adult c-kit[BAC]-EGFP heart 14 days postcryoablation. Note fluorescent cells lining vessel. (*Right*) c-kit-EGFP^{+} endothelial cells lining an artery 7 days postinjury are identified by PECAM1 staining; surrounding smooth muscle cells also express EGFP. (*C*) EGFP[+] cardiomyocytes at border zone. (*Left*) Fluorescent and nonfluorescent striated cardiomyocytes. (*Center* and *Right*) Clusters of EGFP[+] myocytes at border zone 7 days postinfarct. (*D*) Lack of pHH3 in EGFP[+] cardiac myocytes. (*Left*) EGFP[+] and EGFP[−] myocytes at border zone. (*Right*) Single pHH3[+] nonmyocyte within infarct. (Scale bars: *A Left*, 360 μm; *A Right*, 280 μm; *B Left*, 250 μm; *B Inset*, 100 μm; *B Right*, 10 μm; *C*, 22 μm; *D Left*, 14 μm; *D Right*, 16 μm.)

population of cells transitioning from precursor to committed status. Neonatal c-kit^{+} cells are characterized by coexpression of nestin (Fig. 3), a marker of a variety of cells with multilineage potential (15), and some cells express commitment markers (Fig. 2).

FACS sorted c-kit^{+} cells expanded, while differentiating in culture on feeder cells and gelatin-coated plates (Fig. 3). When plated as a mixed (c-kit[+] and c-kit^{−} cells) population, c-kit^{+} cells often formed extended networks next to more compact, contracting cells (Movie S1). EGFP-expressing cells also began to contract in culture and when purified to complete homogeneity by FACS sorting individual fluorescent cells were shown to contract (Movie S3), further demonstrating the mixed differentiation status of c-kit-EGFP^{+} cells. EGFP expression declined gradually in cultured cells, particularly in mixed cultures, indicating the ongoing differentiation of cells in the presence of growth factors such as bFGF.

Many of these cells displayed cardiac-like APs that were sensitive to TTX and had a plateau phase. However, cells also displayed more nodal-like activity without a prominent plateau

phase (Fig. 4). A common characteristic between APs was the presence of a diastolic depolarization phase, which is believed to be generated by a hyperpolarization-activated inward current (I_f) (18). The presence of cells with mixed electrical activity is also a characteristic of ES cell-derived cardiomyocytes and the presence of I_f, I_{Na}, and L-type Ca^{2+} currents in the same cells appears to be a characteristic of cardiac development (16). The plateau phase morphology of some APs and their inhibition by TTX establish the definitive cardiac phenotype of these cells. Vascular smooth muscle cells do not display a characteristic AP feature; it is possible that rhythmically active cells without a plateau phase represent this lineage or, alternatively, that differentiating smooth muscle cells, unlike committed cardiac cells, do not display spontaneous rhythmicity.

After 1 day in culture, a fraction of c-kit^{+} cells stained for either troponin T or αSMA, but despite the identification of PECAM1 staining fluorescent cells in the neonatal heart (Fig. 2), adherent cells were not PECAM1 positive (Fig. 3*G*), whereas after several days in culture PECAM1 was detected (Fig. 3*H*). This may reflect a failure of endothelial-committed cells to

attach or partial digestion of the PECAM1 epitope during enzymatic dissociation.

Our attempts to culture single purified FACS sorted c-kit+ cells resulted in cell death in ES media. Switching to a medium containing bFGF, a growth factor associated with mesodermal cell survival, cell proliferation, and angiogenesis (4), produced viable cells that expanded and produced differentiated mesenchymal cells in culture. Wu et al. (4) also tried to culture FACS sorted Nkx2.5+ cells from 7.5- to 8.5-dpc hearts in similar ES cell media without success. The addition of bFGF appears to be necessary for the propagation of c-kit+ cells in culture (Fig. 5A).

The above results could suggest either the presence of multipotential cardiovascular precursors within the purified cell population, or the selective survival and expansion of precommitted populations under appropriate in vitro conditions. To determine whether c-kit-EGFP+ cells include uncommitted precursors, we undertook clonal analysis by plating cells at limiting dilutions that yielded individual cells within multiwell plates. The absence of attachment factors and conditioning substances resulted in relatively low viability of clones; however, individual surviving cells were observed to expand into clonal colonies and were probed for lineage commitment 21–25 days after plating. Evidence of commitment to all 3 cardiovascular lineages was observed in these clonal populations, although the majority of cells did not express any lineage-specific markers (Fig. 5C). The presence of uncommitted cells within these colonies suggests that the results are not simply explained by expansion of a previously committed cell, that definitive evidence of multilineage potential was obtained by costaining of these clonal populations (Fig. 5D). Differentiation of individual cells to both muscle (cardiac and smooth) and endothelium was observed, definitively establishing the multilineage potential of neonatal c-kit-EGFP+ cells. These results are similar to those reported by Moretti et al. (7), who clonally amplified Isl1+ cells from ED8–8.5 heart cell cultures, and showed that a rare number of these cells differentiated into endothelium, cardiac, and smooth muscle cells. These Isl1+ and/or Nkx2.5+ cells, isolated from hearts at a markedly earlier stage of development, do not express c-kit (15), and our results confirm a lack of Isl1 staining in c-kitBAC-EGFP+ cells.

Recent work (25) demonstrated that pressure overload results in augmented expression of c-kit in cardiomyocytes. Such expression could reflect cardiomyogenesis from c-kit+ CPc, or could be the result of c-kit reexpression in committed myocytes. We show that c-kit expression in the adult injured heart is associated with fibrous and vascular infarct repair, but not myogenesis. C-kit expression is detectable within 3 days postinjury, peaks at 7 days, and declines within a 4-week period to near baseline. EGFP+ expression in cardiomyocytes was only observed in striated, terminally differentiated cells. The lack of EGFP+ myocytes within the infarct zone, absence of immature (nonstriated) troponin T-positive myocytes, and lack of mitotic figures or pHH3 staining in EGFP+ myocytes indicate that cryoinjury does not provoke cardiomyogenesis through activation of c-kit. Rather, these factors indicate that c-kit reexpression occurs in differentiated cardiomyocytes at regions surrounding cardiac injury, activated by local conditions such as hypoxia or inflammatory cytokines, because these cells are not seen at remote regions. Thus, rather than unequivocally identifying adult cardiac precursors, c-kit reexpression in adult cardiac myocytes appears to play a role in the transcriptional activation of fetal/neonatal genes that are induced during cardiac stress (25).

In summary, we describe the purification of a population of cells that includes mesodermally derived cardiovascular precursors, as well as cells in early stages of cardiovascular development. Our results indicate that true CPcs persist through embryonic development and that the PN heart contains significant numbers of these cells, which decline rapidly in the first weeks after birth. Isolated CPcs differentiate into rhythmically contracting cell networks, and individual cells display complex electrical activity. C-kit-EGFP+ cells can be expanded in vitro, although the multipotency of expanded and passaged EGFP+ cells remains to be demonstrated. Finally, c-kit-EGFP+ cells are observed transiently in damaged heart tissue, but do not identify prominent reactivation of resident CPcs in the adult heart. Neonatal c-kit-EGFP+ cells may prove useful for determination of the genetic basis of CPc status and provide a model for the directed differentiation of pluripotent cells for cardiac cell-based therapy.

Materials and Methods

Generation of Tg(RP24-330G11-EGFP)1Mik Mice and Neonatal Heart Characterization. Detailed BAC targeting strategy, PCR genotyping FACS, culturing parameters, electrophysiology, and immunohistochemistry characterization of c-kit-EGFP+ cells are found in *SI Materials and Methods*.

1. Kattman SJ, Huber TL, Keller GM (2006) Multipotent flk-1+ cardiovascular progenitor cells give rise to the cardiomyocyte, endothelial, and vascular smooth muscle lineages. *Dev Cell* 11:723–732.
2. Yang L, et al. (2008) Human cardiovascular progenitor cells develop from a KDR+ embryonic-stem-cell-derived population. *Nature* 453:524–528.
3. Laflamme MA, et al. (2007) Cardiomyocytes derived from human embryonic stem cells in pro-survival factors enhance function of infarcted rat hearts. *Nat Biotechnol* 25:1015–1024.
4. Wu SM, et al. (2006) Developmental origin of a bipotential myocardial and smooth muscle cell precursor in the mammalian heart. *Cell* 127:1137–1150.
5. Beltrami AP, et al. (2003) Adult cardiac stem cells are multipotent and support myocardial regeneration. *Cell* 114:763–776.
6. Urbanek, K., et al. (2006) Stem cell niches in the adult mouse heart. *Proc Natl Acad Sci USA* 103:9226–9231.
7. Moretti A, et al. (2006) Multipotent embryonic isl1+ progenitor cells lead to cardiac, smooth muscle, and endothelial cell diversification. *Cell* 127:1151–1165.
8. Reber L, Da Silva CA, Frossard N (2006) Stem cell factor and its receptor c-Kit as targets for inflammatory diseases. *Eur J Pharmacol* 533:327–340.
9. Yasuda H, Galli SJ, Geissler EN (1993) Cloning and functional analysis of the mouse c-kit promoter. *Biochem Biophys Res Commun* 191:893–901.
10. Alexeev V, Yoon K (2006) Distinctive role of the cKit receptor tyrosine kinase signaling in mammalian melanocytes. *J Invest Dermatol* 126:1102–1110.
11. Andre C, et al. (1997) Sequence analysis of two genomic regions containing the KIT and the FMS receptor tyrosine kinase genes. *Genomics* 39:216–226.
12. Gokkel, E., et al. (1992) Structural organization of the murine c-kit proto-oncogene. *Oncogene* 7:1423–1429.
13. Manova K, et al. (1992) c-kit receptor and ligand expression in postnatal development of the mouse cerebellum suggests a function for c-kit in inhibitory interneurons. *J Neurosci* 12:4663–4676.
14. Laugwitz KL, et al. (2005) Postnatal isl1+ cardioblasts enter fully differentiated cardiomyocyte lineages. *Nature* 433:647–653.
15. Drapeau J, et al. (2005) Nestin-expressing neural stem cells identified in the scar following myocardial infarction. *J Cell Physiol* 204:51–62.
16. Kolossov E, et al. (2005) Identification and characterization of embryonic stem cell-derived pacemaker and atrial cardiomyocytes. *FASEB J* 19:577–579.
17. Gryshchenko, O., et al. (1999) Role of ATP-dependent K(+) channels in the electrical excitability of early embryonic stem cell-derived cardiomyocytes *J Cell Sci* 112(Pt 17):2903–2912.
18. Maltsev VA, et al. (1994) Cardiomyocytes differentiated in vitro from embryonic stem cells developmentally express cardiac-specific genes and ionic currents. *Circ Res* 75:233–244.
19. Roell W, et al. (2007) Engraftment of connexin 43-expressing cells prevents post-infarct arrhythmia. *Nature* 450:819–824.
20. Tallini YN, et al. (2006) BAC transgenic mice express enhanced green fluorescent protein in central and peripheral cholinergic neurons. *Physiol Genomics* 27:391–397.
21. Tallini YN, et al. (2007) Propagated endothelial Ca2+ waves and arteriolar dilation in vivo: Measurements in Cx40BAC GCaMP2 transgenic mice. *Circ Res* 101:1300–1309.
22. Bernex F, et al. (1996) Spatial and temporal patterns of c-kit-expressing cells in WlacZ/+ and WlacZ/WlacZ mouse embryos. *Development (Cambridge, U.K.)* 122:3023–3033.
23. Wouters M, Smans K, Vanderwinden JM (2005) WZsGreen/+: A new green fluorescent protein knock-in mouse model for the study of KIT-expressing cells in gut and cerebellum. *Physiol Genomics* 22:412–421.
24. Fransioli J, et al. (2008) Evolution of the c-kit-positive cell response to pathological challenge in the myocardium. *Stem Cells* 26:1315–1324.
25. Li, M., et al. (2008) c-kit is required for cardiomyocyte terminal differentiation. *Circ Res* 102:677–685.